Electronic Supplementary Material (ESI) for Nanoscale.

Supplementary Information

Highly polarization-sensitive far infrared detector based on optical antenna integrated aligned carbon nanotube film

Binkai Chen, Zhaoyu Ji, Jing Zhou, Yu Yu, Xu Dai, Mengke Lan, Yonghao Bu, Tianyun Zhu, Zhifeng Li, Jiaming Hao, Xiaoshuang Chen

Note1: Comparison between aligned multi-wall carbon nanotube films and aligned single- wall carbon nanotube films for polarization-sensitive far infrared detection

The photoresponse and polarization sensitivity of the aligned multi-wall carbon nanotube (MWCNT) film with or without the optical antenna is investigated. The aligned MWCNT film (Fig. S1 (a)) is regarded as an effective uniaxial material. The fill factor is assumed to be 0.3, the same as that of the SWCNT film presented in the manuscript. The frequency dependent effective permittivity tensor diag ($\varepsilon_x = \varepsilon_\perp$, $\varepsilon_y = \varepsilon_\parallel$, $\varepsilon_z = \varepsilon_\perp$) is evaluated on the basis of real measurements [1]. As shown in Fig. S1 (b), both $\varepsilon_\parallel$ and $\varepsilon_\perp$ almost follow the Drude model since MWCNTs are very conductive in the far infrared regime. The anisotropy originates from the fact that electrons move more freely along the nanotubes than perpendicular to them. As a result, the MWCNTs are more metallic for the light polarized along them than they are for the light polarized perpendicular to them. Correspondingly, $\varepsilon_\parallel$ has a more negative real part and a larger imaginary part than $\varepsilon_\perp$.

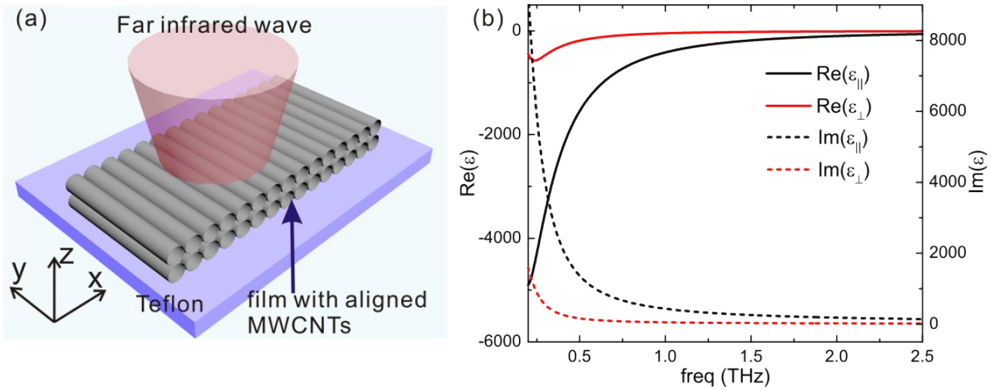

Fig. S1 (a) Sketch of the aligned MWCNT film. (b) Permittivity of the aligned MWCNT film regarded as a uniaxial effective medium.

Then, we replace the aligned SWCNT films with the aligned MWCNT films in the devices with and without the antenna (Fig. S2 (a) and (e)). The rest of the devices all

remain the same. Like the SWCNTs, the MWCNTs are aligned parallel to the *y*-axis and doped diversely to form a p-n junction at the center. The incident light is also assumed to be a Gaussian beam focused on the MWCNT belt with a beam waist around 800 μm. For the device without the antenna (Fig. S2 (a)-(d)), the distribution of the power absorption density (Q_e) almost follows the profile of the Gaussian beam (Fig. S2 (a)-(c)), and then the junction region at the center has a higher temperature than the contacts at the two ends (Fig. S2 (d)), leading to a photoresponse based on the PTE effect. According to previous studies [2], the thermal conductivity along the MWCNTs is evaluated to be ~ 200 W m^{-1} K^{-1} and that perpendicular to the MWCNTs is evaluated to be ~ 60 W m^{-1} K^{-1}. These two values are at the same level with those of the SWCNTs. The heat exchange condition at the air/MWCNT film interface and that at MWCNT film/substrate interface are assumed to be the same as those for the SWCNT film. It is worthy to note that the incident light polarized perpendicular to the MWCNTs ($E \perp y$) induces a much higher light absorption and a much higher temperature rise than the light polarized parallel to the MWCNTs ($E \parallel y$). This polarization dependence is opposite to that of the SWCNT device (Fig. 2 in the manuscript), and it is attributable to the metallic behavior of MWCNTs. For $E \perp y$, the aligned MWCNT film works like a good conductor and hence a lot of power is reflected. For $E \perp y$, the aligned MWCNT film becomes less conductive so light could penetrate further into the material, leading to more prominent power dissipation. The typical Seebeck coefficients for p-doped and n-doped MWCNTs are around 15 μV/K and -15 μV/K, respectively [3]. Based on that, the responsivity for the $E \perp y$ and $E \parallel y$ are estimated to be 13 V/W and 0.034 V/W, respectively. Then, the polarization extinction ratio (PER) for responsivity is about 382. For the antenna integrated device (Fig. S2 (e)-(h)), when the incident light is polarized along the *y*-axis ($E \parallel y$), the

bowtie antenna concentrates the power into the gap that overlaps the junction region (Fig. S2 (b) top row), and induces a local absorption enhancement (Fig. S2 (g) red line) and a local temperature rise (Fig. S2 (h) red line). However, since the aligned MWCNT film is quite conductive for this polarization, the antenna load is too small to match the impedance, so a lot of power is scattered and the local field intensity is not very significant. For $E \perp y$, the antenna does not concentrate the light in the gap but at the corners, so the junction region becomes an absorption valley. As revealed by Fig. S2 (f) and (g), within the antenna aperture, the absorption of the MWCNTs are reduced, while out of the antenna aperture, the absorption of the MWCNTs recovers to the same level as that in the absence of the antenna. The junction temperature still rises up due to heat transfer, and it is 13 times higher than that for $E // y$ since the aligned MWCNTs absorbs the light with $E \perp y$ much more efficiently. Then, the responsivity for $E \perp y$ and $E // y$ are estimated to be 5.34 V/W and 0.41 V/W, respectively. The PER for the responsivity is about 13.

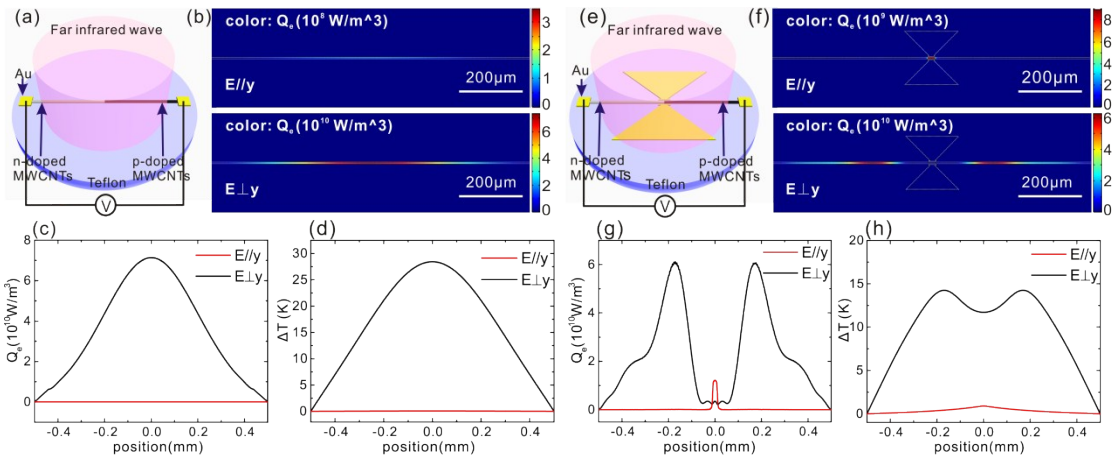

Fig. S2 (a) Sketch of the infrared photodetector based on the aligned MWCNT belt. (b) Distributions of the light power absorption density (Q_e) for the y- and x-polarization on the x-y cross-section at z = 1 μm (i.e. half thickness of the MWCNT film). (c) Line profiles of Q_e along the x-direction and through the center of the MWCNT film (y = 0 μm, z = 1 μm) for the x- and y-polarization. (d) Line profiles of ΔT along the x-

direction and through the center of the MWCNT film for the *x*- and *y*-polarization. (e)-(h) present the sketches and the quantities in the same way as (a)-(d) for the bowtie antenna integrated aligned MWCNT belt. The dimensions of the MWCNT belt and the antenna all follow the SWCNT devices presented in Fig. 2 in the manuscript.

Fig. S3 presents the spectra of absorptance and responsivity for the MWCNT devices with and without the antenna. For $E \,//\, y$, the antenna improves the absorptance and the responsivity at the resonance, while for $E \perp y$, it reduces the absorptance and the responsivity. This behavior has already been revealed during our investigation on the SWCNT devices, as shown in Fig. 3 in the manuscript. In that case, the double-dealing behavior benefits the PER. However, the current situation is just the opposite. Since the absorptance of the aligned MWCNTs for $E \perp y$ is much lower than that for $E \,//\, y$, the improvement of responsivity for $E \,//\, y$ and the suppression of that for $E \perp y$ degrades the PER seriously. As shown in Fig. S3 (b), the integration of the antenna degrades the PER from 382 to 13 at the resonance around 1 THz.

Consequently, in the case of the aligned MWCNT film, the integration of an optical antenna does not enhance but degrades the PER for responsivity. For the MWCNT device without the antenna, the PER (382 at 1 THz) is not as high as that of the SWCNT device with the antenna (1753 at 1 THz). Moreover, since the Seebeck coefficients of the MWCNT film is not as high as those of the SWCNT film, the absolute responsivity of the MWCNT film based device is lower by more than 6 times. Therefore, the antenna integrated aligned SWCNT film is more favorable for highly polarization-sensitive far infrared detection.

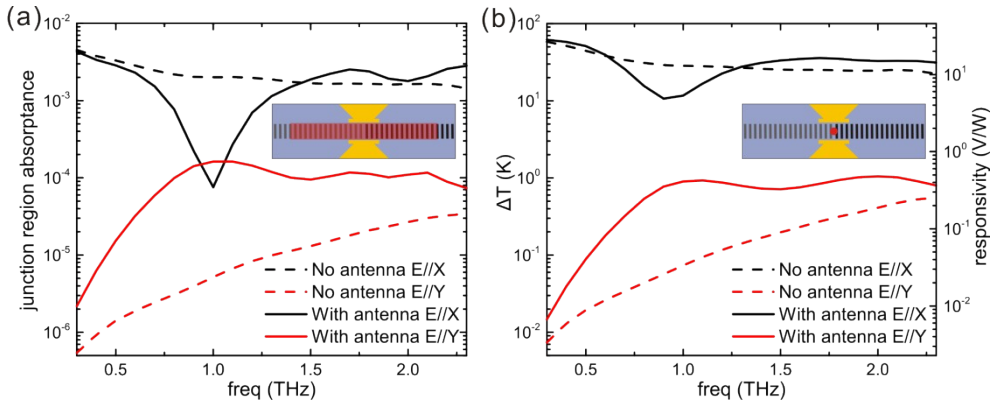

Fig. S3 (a) Junction region absorptance spectra of the antenna integrated MWCNT belt and the MWCNT belt without the antenna for the *x*- and *y*-polarized incident light. The junction region, as sketched by the red shadow in the inset, is defined as a 5 μm × 100 μm rectangle at the center of the MWCNT belt. (b) Spectra of temperature increase at the junction (ΔT) and responsivity of the antenna integrated MWCNT belt and the MWCNT belt without the antenna for the *x*- and *y*-polarized incident light.

Note2: Key parameter comparison between the device we propose and those in other works

The key parameters including polarization sensitivity, responsivity, and detectivity are compared with other works quantitatively. The PERs for responsivity of the photodetectors based on aligned CNT films are typically below 5 [4,5], and the PER of the antenna integrated aligned SWCNT belt as we propose is predicted to be higher than 700 over a wide frequency range from 0.5 to 1.5 THz. And the maximum value exceeds 13600. The responsivity of a photodetector based on an aligned SWCNT film is around 1.25 V/W for THz waves [4]. In comparison, the peak responsivity of our antenna integrated aligned SWCNT belt is 75 V/W in average in the THz regime. The detectivity can be expressed by the noise equivalent power (NEP). The NEP of a photodetector based on an aligned SWCNT film is around 20 $nW/Hz^{1/2}$ [4]. The resistance of our device, where the SWCNT belt is 5 μm wide and 1 mm long, is

estimated to be 3 MΩ [4,6]. For the detectors based on the PTE effect, the noise is primarily thermal and it can be expressed as $\sqrt{4k_BTR}$ [7]. Then, the NEP of our device is estimated to be 2.9 nW/Hz$^{1/2}$. Therefore, with the help of the antenna, all the key parameters are improved, and especially the polarization sensitivity can approach an ultra-high level.

Referecnes:

[S1]Y. Wang, G. Duan, L. Y. Zhang, L. H. Ma, X. G. Zhao, and X. Zhang, "Terahertz Dispersion Characteristics of Super-aligned Multi-walled Carbon Nanotubes and Enhanced Transmission through Subwavelength Apertures", Sci. Rep. 8, 2087 (2018).

[S2]L. Qiu, X. T. Wang, G. P. Su, D. W. Tang, X. H. Zheng, J. Zhu, Z. G. Wang, P. M. Norris, P. D. Bradford, Y. T. Zhu, "Remarkably enhanced thermal transport based on a flexible horizontally-aligned carbon nanotube array film", Sci. Rep. 6, 21014 (2016).

[S3]Y.-M. Choi, D.-S. Lee, R. Czerw, P.-W. Chiu, N. Grobert, M. Terrones, M. Reyes-Reyes, H. Terrones, J.-C. Charlier, P. M. Ajayan, S. Roth, D. L. Carroll, Y.-W. Park, "Nonlinear Behavior in the Thermopower of Doped Carbon Nanotubes Due to Strong, Localized States", Nano Lett. 3, 839-842(2003).

[S4]X. W. He, N. Fujimura, J. M. Lloyd, K. J. Erickson, A. A. Talin, Q. Zhang, W. L. Gao, Q. J. Jiang, Y. Kawano, R. H. Hauge, F. Leonard, J. Kono, "Carbon Nanotube Terahertz Detector", Nano Lett. 14, 3953−3958 (2014).

[S5]X. He, X. Wang, S. Nanot, K. Cong, Q. Jiang, A. A. Kane, J. E. M. Goldsmith, R. H. Hauge, F. Léonard, and J. Kono, "Photothermoelectric p-n Junction Photodetector with Intrinsic Broadband Polarimetry Based on Macroscopic Carbon Nanotube Films", ACS Nano 7, 7271-7277 (2013).

[S6]Q. Cao, H. Kim, N. Pimparkar, J. P. Kulkarni, C. Wang, M. Shim, K. Roy, M. A. Alam, J. A. Rogers, Medium-scale carbon nanotube thin-film integrated circuits on flexible plastic substrates, Nature 454, 495 (2008).

[S7]Q. Zeng, S. Wang, L. Yang, Z. Wang, T. Pei, Z. Zhang, L.-M. Peng, W. Zhou, J. Liu, W. Zhou, S. Xie, Carbon nanotube arrays based high-performance infrared

photodetector, Opt. Mater. Express 2, 839 (2012).